PERGAMON

International Journal of Heat and Mass Transfer 42 (1999) 4185–4195

International Journal of HEAT and MASS TRANSFER

www.elsevier.com/locate/ijhmt

Natural convection in a cylindrical porous cavity with internal heat source: a numerical study with Brinkman-extended Darcy model

H. Jiménez-Islas, F. López-Isunza*, J.A. Ochoa-Tapia

Departamento de Ingeniería de Procesos e Hidráulica, Universidad Autónoma Metropolitana-Iztapalapa, Ave Michoacán y La Purísima s/n, Col. Vicentina, Delegación Iztapalapa, CP 09340, México, D.F. Mexico

Received 21 January 1998; received in revised form 12 February 1999

Abstract

Natural convection in a 2-D vertical cylinder containing an isotropic porous media with internal heat generation was studied numerically for assessing the effect of Darcy's law with and without the Brinkman extension on the streamlines, isotherms and Nusselt numbers. Two cases were analyzed: (1) insulated walls at the top and bottom of the cylinder and cooled external walls; (2) isothermally cooled walls at all external surfaces. The effect of the Brinkman extension was significant for high values of Da (10^{-4}–10^{-1}). In addition, the Nusselt number increases asymptotically as Da decreases. Also, four correlations for the average Nusselt number were derived.

1. Introduction

The phenomena of natural convection in a cylinder containing a saturated porous media with internal heat generation, has been analyzed in great detail in the last ten years, due to the various applications in engineering [1,2], particularly in the study of grain and cereal storage, drying and fumigation in silos, where important problems to analyze are related to the effect of the metabolic heat generation in grains, causing hot spots that induce fungal growth, grain germination or the proliferation of insects [1,3]. Other important applications deal with heat transfer studies in the confinement of nuclear wastes, and the analysis and design of fixed-bed catalytic reactors. Many studies on natural convection have been published in the literature, and the papers by Havstad and Burns [4], Prasad and Chui [5], David et al. [6], Hunt and Tien [7], and Chang and Hsiao [8], are related to this work. All of these use Darcy's law to describe the flow in the porous media, despite this approach does not satisfy the non-slip conditions, neglecting inertial effects when they may become important.

The utilization of Darcy's law implies fluid slip at the walls, since it lacks a diffusive term that considers the distortion of the velocity profiles near a solid boundary. Brinkman [9] suggested that a second-order term, $\mu\nabla^2$, could be added to the Darcy's law to account for the energy losses due to viscous transport, considering the distortion of the streamlines in the proximities of impermeable rigid walls. In this form, Brinkman's extension allows the use of a non-slip condition at the solid wall, which becomes important in the study of the behavior of high porosity porous media, although, in many cases the effect of viscous

* Corresponding author. Tel.: +52-5-724-4956; fax: +52-5-724-4900.

E-mail address: felipe@xanum.uam.mx (F. López-Isunza)

0017-9310/99/$ - see front matter
PII: S0017-9310(99)00065-4

Nomenclature

A	height/radius ratio aspect, L/R
Da	Darcy number, K/R^2
K	permeability of the porous medium, m^2
L	height of cylindrical cavity, m
Nu	Nusselt number, $h_c R/k$
R	cylinder radius, m
Ra	Rayleigh number for the porous medium, $g\rho\beta KSR^3/(2\mu\alpha k)$
S	volumetric heat source, W/m^3
u	dimensionless velocity, $v_r R/\alpha$, $v_z R^2/\alpha L$.

Greek symbols

ζ	dimensionless axial coordinate, z/L
θ	dimensionless temperature $(T-T_c)/(SD^2/2k)$
ξ	dimensionless radial coordinate, r/R
ψ	dimensionless stream function
ω	dimensionless vorticity.

Subscripts

c	cooled wall
max	maximum value
med	average value
r	radial direction
z	axial direction.

transport is negligible (porous media with Darcy's number, $Da < 10^{-4}$). Ochoa-Tapia and Whitaker [10] have proposed a jump condition to couple Darcy's law and the Brinkman extension to the Stokes equation, obtaining a continuous volume-averaged velocity field. This provides a theoretical support to the Darcy's law for the use of a non-slip criterion, and for the coupling of equations at inter-regional boundaries occurring in systems with porous medium–fluid interfaces, like those at the upper part in a silo [2,9]. On the other hand, Lauriat and Prasad [11] showed that the Nusselt number decreases as the Darcy number increases above 10^{-5}, while maintaining constant the Rayleigh number and the geometric aspect ratio. Kladias and Prasad [12] studied the natural convection in a horizontal porous layer heated from below, employing Darcy's law with the Brinkman–Forchheimer extension. They found that for $Da < 10^{-5}$, Nu remains almost unchanged, however its value increases as $Da > 10^{-5}$, approaching to an asymptotic value at larger Da.

The objective of this work is to investigate the effect of the Brinkman extension on Darcy's law, in the study of natural convection, for two different boundary conditions, in a two-dimensional cylindrical saturated porous cavity with internal heat generation, for $10^{-10} \leq Da \leq 10^{-1}$. This includes the range of importance of viscous dissipation ($10^{-4} < Da < 10^{-1}$), up to the limit when inertial effects become important ($Da > 10^{-1}$). The conservation equations are solved using orthogonal collocation, and the results are compared with those obtained previously by Prasad and Chui [5].

2. Mathematical formulation and numerical methods

The geometrical system under study is a vertical cylindrical cavity of radius R and height L, containing an isotropic and saturated porous media with uniform volumetric heat generation, as shown in Fig. 1. Assuming that the external walls of the cylinder are kept to a constant temperature T_c, two cases are analyzed:

1. Adiabatic horizontal walls.
2. Isothermally cooled horizontal walls.

Because of the symmetry of velocity and temperature profiles with respect to the axial axis of the cylinder, only the region between $0 < r < R$ and $0 < z < L$ is considered. Moreover, the model is based on the following assumptions:

1. Effective isotropic medium with constant thermodynamic properties, where viscosity and density correspond to that of the fluid, using an effective thermal conductivity for the porous medium.
2. The porous medium is a cavity with rigid impermeable walls, therefore there is no fluid slip.
3. The interstitial fluid is Newtonian, moving in laminar flow, and the system is at steady state.

The corresponding dimensionless conservation equations are obtained by applying the curl to the momentum equation, eliminating the pressure term [5], together with the use of the stream function and vorticity criteria [13]:

Vorticity:

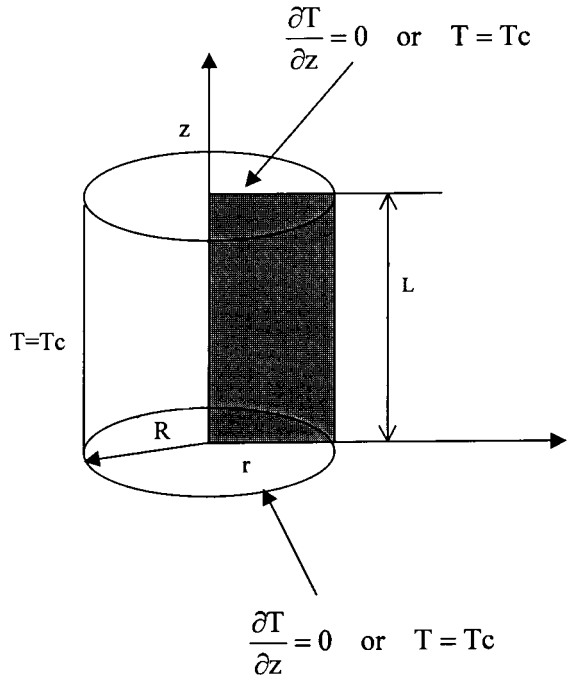

Fig. 1. Geometric system used in this work, with axial symmetry.

$$\omega = \frac{A^2}{\xi}\frac{\partial^2\psi}{\partial\xi^2} - \frac{A^2}{\xi^2}\frac{\partial\psi}{\partial\xi} + \frac{1}{\xi}\frac{\partial^2\psi}{\partial\zeta^2} \tag{1}$$

Momentum equation:

$$\omega = Da\left[\frac{\partial^2\omega}{\partial\xi^2} + \frac{1}{\xi}\frac{\partial\omega}{\partial\xi} + \frac{1}{A^2}\frac{\partial^2\omega}{\partial\zeta^2} - \frac{\omega}{\xi^2}\right] + Ra\frac{\partial\theta}{\partial\xi} \tag{2}$$

Energy:

$$\frac{1}{\xi}\frac{\partial\psi}{\partial\xi}\frac{\partial\theta}{\partial\zeta} - \frac{1}{\xi}\frac{\partial\psi}{\partial\zeta}\frac{\partial\theta}{\partial\xi} = \frac{\partial^2\theta}{\partial\xi^2} + \frac{1}{\xi}\frac{\partial\theta}{\partial\xi} + \frac{1}{A^2}\frac{\partial^2\theta}{\partial\zeta^2} + 2 \tag{3}$$

In these expressions, the dimensionless velocities u_r and u_z are defined in terms of the stream function ψ as:

$$u_r = -(1/\xi)\,\partial\psi/\partial\zeta \quad u_z = (A^2/\xi)\,\partial\psi/\partial\xi \tag{4a,b}$$

The corresponding boundary conditions for the steam function and dimensionless temperature are:

$$\xi = 0, \quad \psi = 0, \quad \partial\theta/\partial\xi = 0 \tag{5a}$$

$$\xi = 1, \quad \psi = 0, \quad \theta = 0 \tag{5b}$$

$$\zeta = 0, \quad \psi = 0, \quad \partial\theta/\partial\zeta = 0 \quad \text{or } \theta = 0 \tag{5c}$$

$$\zeta = 1, \quad \psi = 0, \quad \partial\theta/\partial\zeta = 0 \quad \text{or } \theta = 0 \tag{5d}$$

On the other hand, Wood's approximation [13] was used to obtain the boundary conditions for the vorticity term in the momentum equation. The system of nonlinear elliptic PDE, Eqs. (1)–(3), was discretized using the method of orthogonal collocation [14]. The number of interior collocation points selected were: 13×13 for low values of the Rayleigh number, and up to 25×25 for high values of Ra ($>10^4$), due to the increasing effect of the buoyancy forces as Ra increases, consequently, increasing the distortion of the isotherms at the boundaries, a well-known source for numerical instability [5]. The set of nonlinear algebraic equations was solved either by using a quasi-Newton method with LU factorization, or by using nonlinear relaxation (NLR), via the code ELI-COL [15]. The accuracy of the numerical solution was verified by performing a global energy balance that compares the heat generated internally versus the heat removed throughout the external walls of the cylinder.

3. Results and discussion

For the case of natural convection considered in this study buoyancy forces are produced by the heat generated at the solid phase, and this term has been included in the definition of the Rayleigh number (Ra). For values of $Ra < 10$ the conductive effect dominates, while for greater values of Ra the generated heat together with the cooling at the external walls of the cylinder, induce density gradients in the interstitial fluid, causing fluid motion. The rate of this motion increases as the Rayleigh number increases, due to an increase in heat transfer; therefore, it is expected that the Nusselt number (Nu) will be a direct function of Ra.

As mentioned before, two cases are considered in this study. Of particular interest is case two, for which predictions of bicellular flow with Darcy's law are not found when the Brinkman extension is used, as shown below.

3.1. Case I. Insulated top and bottom walls

For this case the numerical simulations consider the parameter range: $0 \le Ra \le 25{,}000$; $0.5 \le A \le 5.0$ and $10^{-10} \le Da \le 10^{-1}$. Inside the range for the Darcy's number, viscous effects become more important as Da approaches the value of 10^{-1}, on the other hand, inertial effects become important when $Da > 10^{-1}$, and the porosity of the solid medium approaches the value of 1.

Fig. 2 shows the effects of the varying Darcy's number, when $Da = 10^{-1}$, 10^{-2}, 10^{-6} and 10^{-10}, on flow

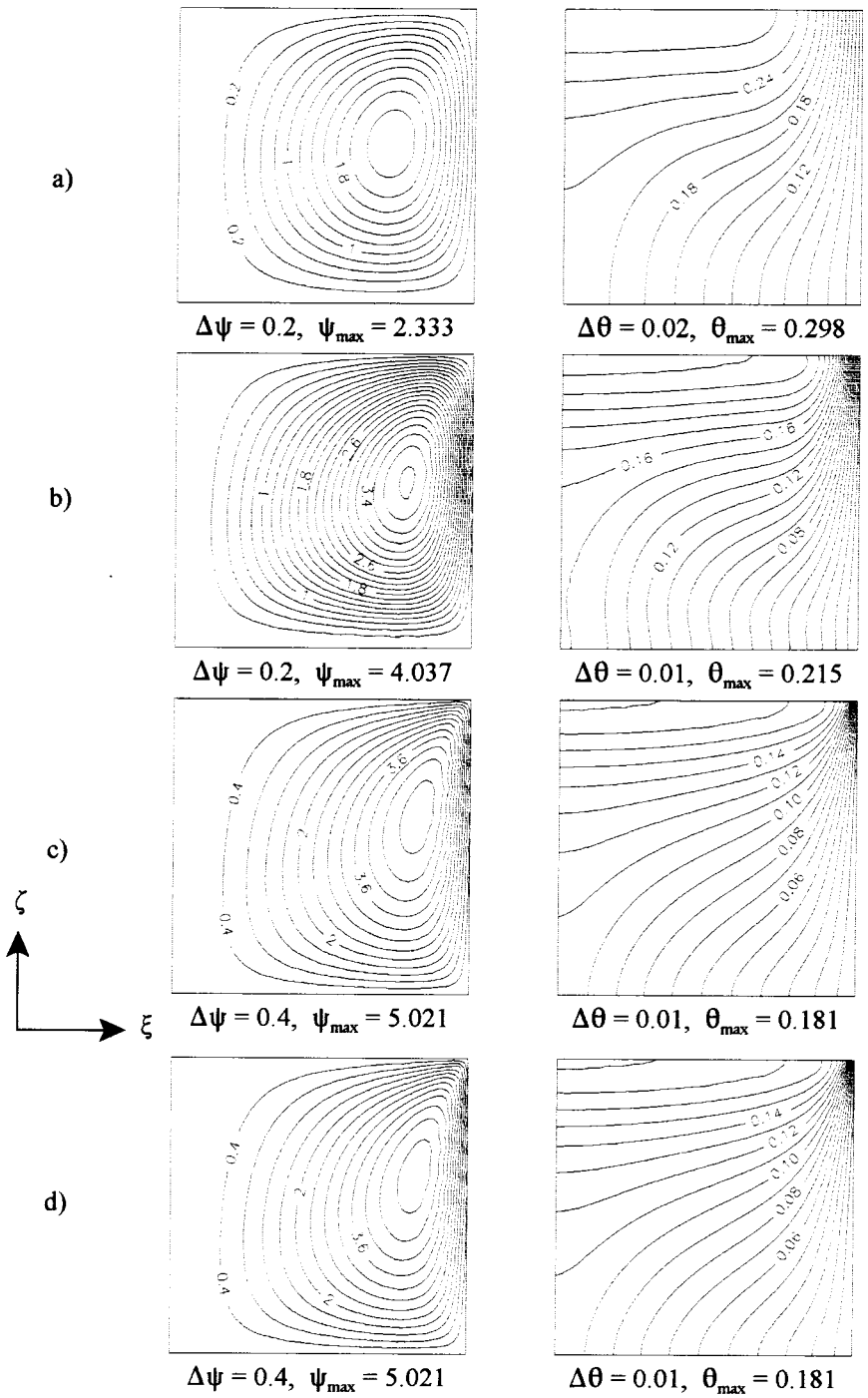

Fig. 2. Effect of the Darcy number on flow patterns and isotherms at $A = 1$ and $Ra = 1000$ for insulated top and bottom. (a) $Da = 10^{-1}$, (b) $Da = 10^{-2}$, (c) $Da = 10^{-6}$, (d) $Da = 10^{-10}$.

patterns and isotherms, for $Ra = 1000$ and $A = 1$. It can be observed that for $Da = 10^{-1}$ (Fig. 2(a)), the flow moves slowly, isotherms present its maximum values and the heat transfer rate is the lowest, as compared to those for $Da = 10^{-6}$ and $Da = 10^{-10}$ (Fig. 2(c) and (d)), for which almost no variation is found in fluid velocity and temperature profiles, as viscous effects become negligible. This is an important difference between the predictions obtained with and without Brinkman's extension to the Darcy's law for this case, as Darcy's law will predict a similar behavior for the case in Fig. 2(a) as those for cases 2(b)–(d). For the case of $Ra = 5000$, the flow moves faster than for $Ra = 1000$, therefore, the isotherms exhibit lower

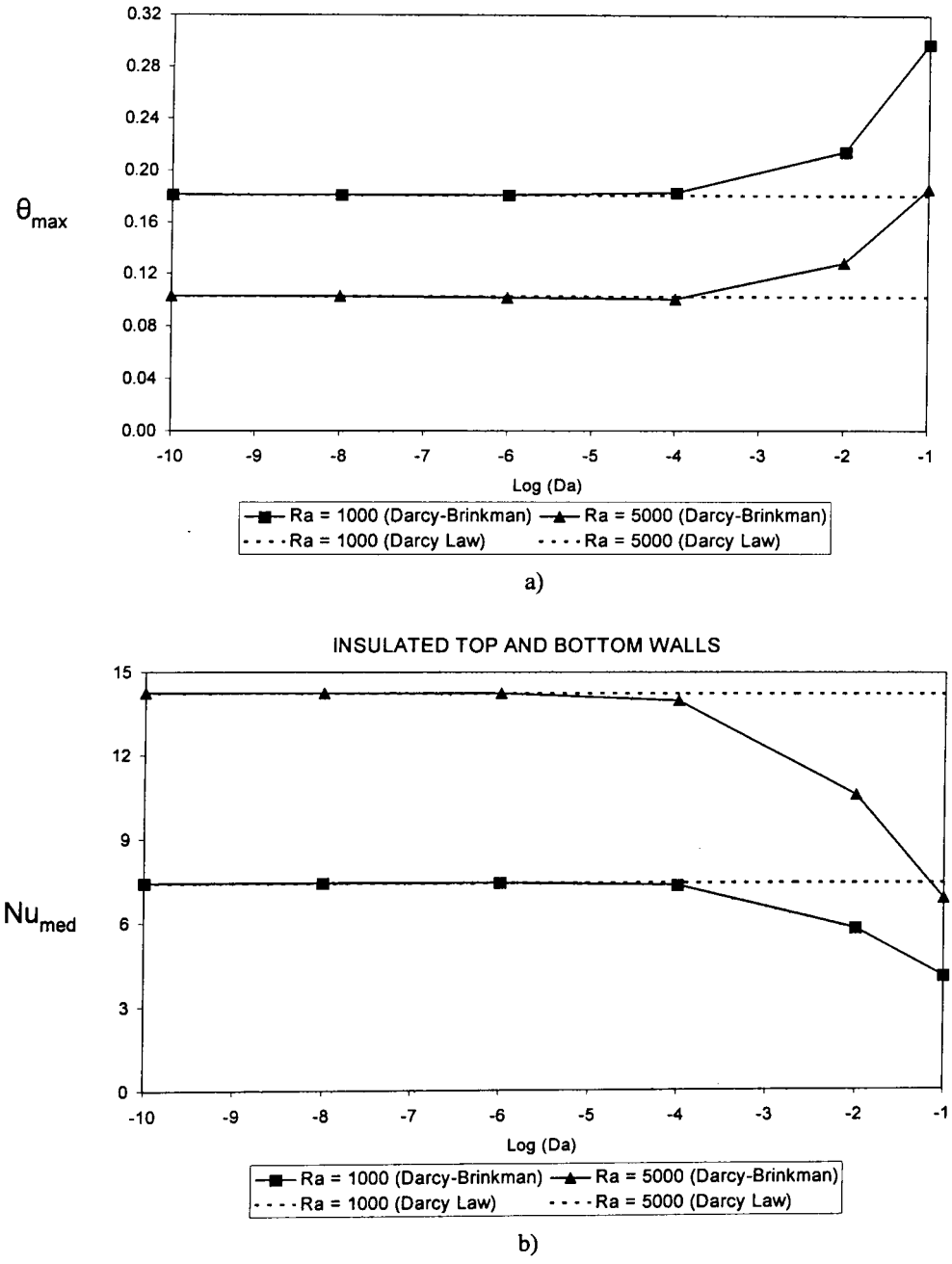

Fig. 3. Behavior of (a) θ_{max} and (b) the average Nusselt number versus the Darcy number for insulated top and bottom walls.

Table 1
Comparison between Nu_{med} estimated from Eq. (7) and Nu_{med} calculated numerically

Ra	*A*	*Da*	Nu_{med} Eq. (7)	Nu_{med} numerical	% Error
575	155	5.75×10^{-7}	4.531	4.766	4.95
2383	83	1.23×10^{-4}	10.236	9.926	3.12
25,000	100	1.00×10^{-8}	25.703	26.811	4.13

values due to a larger cooling throughout the vertical walls. A similar behavior was reported by Lauriat and Prasad [11] in their study of a rectangular enclosure with insulated horizontal walls.

In summary, the value of $Da = 10^{-4}$ represents the limit where viscous effects are important in a porous medium, and this becomes practically Darcian as *Da* is further reduced. This has already been pointed out by several authors [11,12] for other geometries and has also been found for this geometric system.

3.1.1. Global heat transfer

To evaluate the heat transfer throughout the walls a difference between the average temperature at the axial axis of the cylinder (T_{med}) and the external wall temperature (T_c) has been used. Then, as a result of the global energy balance, the average Nusselt number is defined as:

$$Nu_{med} = \frac{1}{\theta_{med}} \tag{6}$$

Based on the values of θ_{max}, θ_{med} and Nu_{med} obtained, we concluded that in a pure conductive regime (i.e., $Ra = 0$), $Nu_{med} = 2$ for all values of *A* and *Da*. Figs. 3(a) and (b) compare model prediction using Darcy's law with and without Brinkman's extension term, showing the dependency of θ_{max} and Nu_{med} as a function of *Da*, for $Ra = 1000$ and $Ra = 5000$. Again, the inclusion of the Brinkman extension term to the Darcy's law shows a different behavior for θ_{max} and Nu_{med}, when $10^{-4} < Da < 10^{-1}$. The value of θ_{max} remains practically constant for $Da < 10^{-4}$, increasing afterwards for $10^{-4} < Da < 10^{-1}$ when viscous effects become important. In the case of Nu_{med}, it shows an opposite behavior as *Ra* increases. As expected, θ_{max} is always located at the center of the top surface. An empirical expression has been obtained for Nu_{med}, in terms of the Darcy and Rayleigh numbers and the aspect ratio *A*, as follows:

$$Nu_{med} = 0.4132 Ra^{0.3884} A^{-0.4857} Da^{-0.01063} \tag{7}$$

The relation is valid in the range: $100 \leq Ra \leq 10{,}000$, $0.5 \leq A \leq 5.0$, $10^{-2} \leq Da \leq 10^{-10}$. The maximum error obtained was 12% using values of *Ra, A* and *Da*, with an average error of 5.94%. Eq. (7) cannot be used for values of $Da = 10^{-1}$, due to the large error obtained (25%), suggesting that the behavior in this region is more complex, as inertial effects becomes important. In comparison, the correlation obtained using the results from Darcy's law is given by:

$$Nu_{med} = 0.3958 Ra^{0.4168} A^{-0.4654} \tag{8}$$

Valid in the range: $100 \leq Ra \leq 10{,}000$ and $0.5 \leq A \leq 5.0$, with an average error of 5.09%. Table 1 compares the values of Nu_{med} from Eq. (7) with those obtained from the numerical simulations, for selected values of *Ra, A* and *Da*. Table 1 also shows that predictions of the Nusselt number from Eq. (7) are good, even for values of $Ra = 25{,}000$. This confirms the fact that the flow, under these boundary conditions, is stable and unicellular. Prasad and Chui [5] reported values of Nu_{med} for $A = 1$, 5 and 20. The first two cases are compared with results obtained in this work and are given in Table 2 for $Da = 10^{-10}$, considering that the flow is Darcian [5]. Finally, Fig. 4 compares the variation of Nu_{med} as a function of *Ra* for $\{A = 1,\ Da = 10^{-8}\}$ and $\{A = 5,\ Da = 10^{-10}\}$,

Table 2
Values of Nu_{med} for selected values of *Ra* and *A*

Ra	*A*	Nu_{med} Prasad and Chui [5]	Nu_{med} numerical	Nu_{med} Eq. (7)
100	1	3.155	3.096	3.157
1000	1	7.639	7.435	7.721
10,000	1	19.841	18.762	18.883
100	5	2.513	2.107	1.445
1000	5	5.695	3.608	3.553
10,000	5	14.006	7.979	8.641

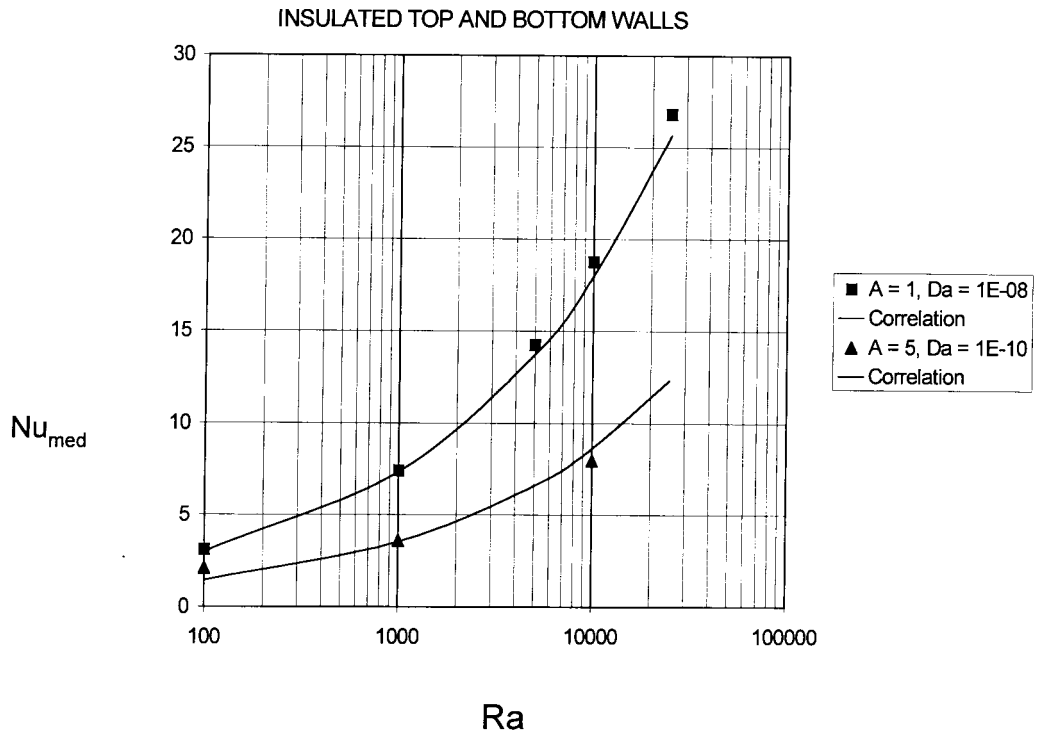

Fig. 4. Comparison of Eq. (7) with numerical values of average Nusselt number as a function of the Rayleigh number for insulated top and bottom walls.

evaluated with Eq. (7) with those from the numerical simulations. It can be observed that, as A increases because of the increase in the height of the cylinder, the effect of the buoyancy forces decrease, reducing Nu_{med}.

The accuracy of the orthogonal collocation method was successfully tested, obtaining a maximum error 1.97% in the global energy balance closure. Some of the parameters like *Ra, A* and *Da*, were selected to be the same as those reported by Prasad and Chui [5], to have a basis for comparison. Also, in this way, the contribution of the Brinkman extension term has been assessed.

3.2. Case II. Exterior walls isothermally cooled

For this case, the numerical simulations were performed in the parameter range: $0 \leq Ra \leq 10{,}000$, $0.5 \leq A \leq 5.0$ and $10^{-10} \leq Da \leq 10^{-1}$. Fig. 5 shows streamlines and isotherms when $Ra = 5000$ and $A = 1$ for $Da = 10^{-1}$, 10^{-2}, 10^{-4} and 10^{-10}. As in the previous case, the predictions show that the flow rate increases as Da decreases, until the limiting value of 10^{-4} is reached, with apparently no further increase as Da is reduced to 10^{-10}. The corresponding isotherms show again larger temperatures when $Da = 10^{-1}$, as a result of the slower fluid motion. Furthermore, bicellular flow is predicted (Figs. 5(c) and (d)) for $Da < 10^{-4}$, which is in agreement with the work of Prasad and Chui [5]. The difference observed between the predicted temperature and streamline profiles in Figs. 5(a) and (b) with those from Figs. 5(c) and (d) are due to the Brinkman's extension term in the Darcy's law, which plays no role in the last two cases, but becomes important in Figs. 5(a) and (b).

3.2.1. Global heat transfer

The Nusselt number is defined in terms of a global energy balance, as in Case I, i.e., considering the difference between T_{med} and T_c. Because for this case T_{max} is not located at the axial axis, it is necessary to calculate T_{med} by a discrete integration. The expression is:

$$Nu_{med} = \frac{A}{(A+1)\theta_{med}} \tag{9}$$

Eq. (9) shows that Nu_{med} depends on the geometric aspect ratio, and it can be observed that as the height of the cylinder increases, the heat transfer throughout the walls decreases. This can be compared with Eq. (6) for Case I, where Nu_{med} is not given as an explicit function of the geometrical aspect ratio. The variation of Nu_{med} with respect to *Ra, A*, and *Da* presents an

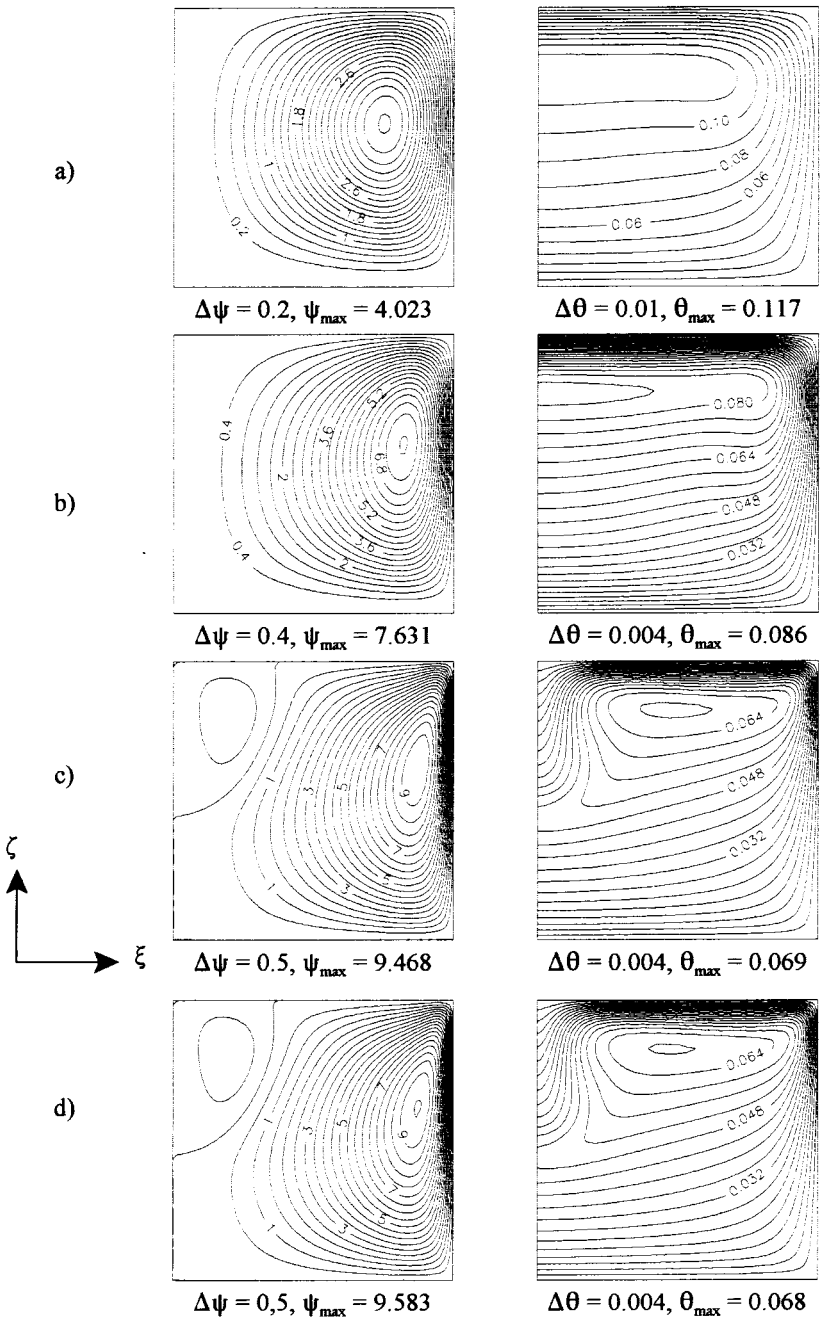

Fig. 5. Effect of the Darcy number on flow patters and isotherms at $A = 1$ and $Ra = 5000$ for isothermally cooled walls. (a) $Da = 10^{-1}$, (b) $Da = 10^{-2}$, (c) $Da = 10^{-4}$, (d) $Da = 10^{-10}$.

analogous behavior as in Case I. On the other hand, comparing Cases I and II (top and bottom surfaces insulated and cooled walls, respectively), Nu_{med} is greater in the second case due to the larger heat removal because of the allowance for a greater heat transfer area due to the boundary conditions.

Figs. 6(a) and (b) show the behavior of $\theta_{\max}$ and Nu_{med}, as a function of Da, for $Ra = 1000$ and

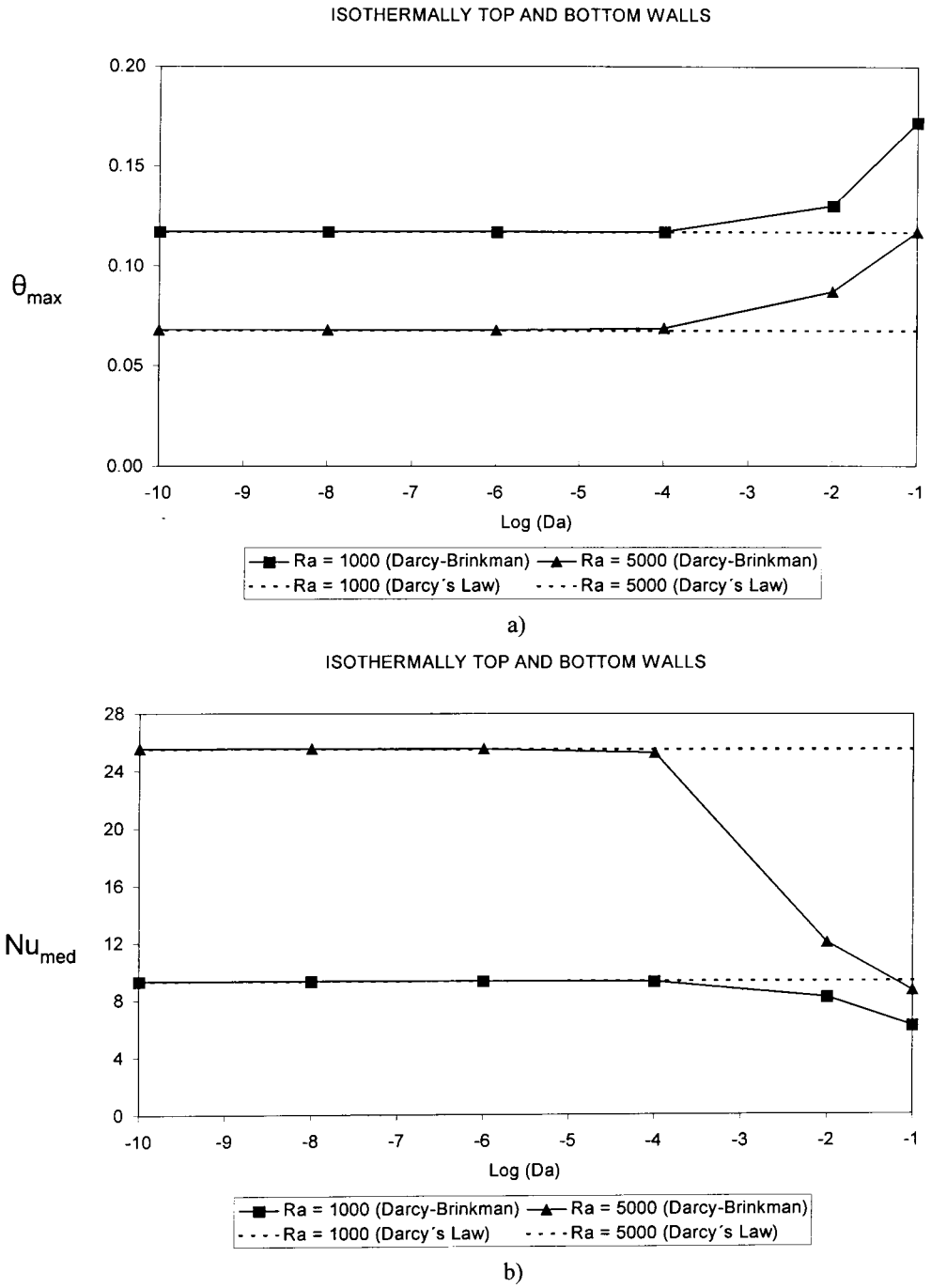

Fig. 6. Behavior of (a) θ_{max} and (b) the average Nusselt number versus the Darcy number for isothermally cooled walls.

$Ra = 5000$. The magnitude of θ_{max} remains practically constant for $Da = 10^{-4}$, increasing afterwards. In the case of Nu_{med}, the inverse behavior is observed. The explanation for these phenomena has been described previously; in addition to this, the behavior of θ_{max} and Nu_{med} are related to the viscous transport region ($Da > 10^{-4}$) and the Darcy-flow region ($Da < 10^{-4}$). It is important to say that, in this case, θ_{max} is located within the region defined by: $0 > \xi < 1$ and $0.5 < \xi < 1$.

Table 3
Comparison between values of Nu_{med} estimated with Eq. (10) calculated by numerical simulation

Ra	A	Da	Nu_{med} Eq. (10)	Nu_{med} numerical	% Error
623	2.3	0.0080	4.964	5.096	2.59
323	4.0	0.0200	3.176	3.333	4.73
1500	0.8	0.0003	10.803	10.093	6.55
52	4.0	0.0200	2.123	2.850	25.40

For prediction purposes, a correlation was developed for Nu_{med} in terms of Ra, A, Da, by a nonlinear regression, yielding the following expression:

$$Nu_{med} = 1.837 Ra^{0.2204} A^{-0.5376} Da^{-0.00492} \quad (10)$$

The validity range for Eq. (10) is: $100 < Ra < 1000$; $0.5 < A < 5.0$ and $10^{-10} < Da < 10^{-1}$. Comparing the predicted values with those numerically obtained, a maximum error of 5.35% was found, with an average error of 2.68%. The parameter range in this case is narrower than the one for Eq. (7), which may be explained by the flow-transition effects in the porous media (inertial effects), that are manifested at $Da = 10^{-1}$. Also, we obtained the following expression for the Nusselt number with the results for Darcy's law:

$$Nu_{med} = 2.0497 Ra^{0.2163} A^{-0.5122} \quad (11)$$

The validity range for Eq. (11) is: $100 < Ra < 1000$ and $0.5 < A < 5.0$, with an average error of 2.52%. On the other hand, Table 3 presents an evaluation of the usefulness of Eq. (10) for predicting Nu_{med}, using parameter values of: Ra, A and Da not used previously in the computer simulations. A comparison of the Nu_{med} values is presented with those obtained by the numerical solution of the conservation equations, even for those cases which are outside of the validity range of Eq. (10).

4. Conclusions

A numerical study is presented on the natural convection inside a closed cylinder containing an isotropic porous media with internal heat generation, to assess the importance of Brinkman's extension included in the Darcy's law in the region where the viscous effects are important ($10^{-4} < Da < 10^{-1}$). The incorporation of this term allows the flow analysis in the porous medium when the solid matrix is sparse (high values of Da). In this way, the viscous effects can also be evaluated as they are manifested on the solid–fluid interface. Furthermore, it allows one to support, mathematically, the non-slip conditions on rigid and impermeable walls, that constitute most of the boundary conditions in engineering application problems.

The effect of the Darcy number is important for values in the range 10^{-1}–10^{-4}, becoming negligible for smaller values, showing the validity of the Darcy's law within this range, for the geometric system considered in this study and the like reported elsewhere in the literature. In Case I, the Nusselt number increases by reducing Da, approaching to a limiting value when $Da = 10^{-4}$. For Case II, a similar situation is observed, but the magnitude of Nu_{med} is greater. On the other hand, for values of Da near 10^{-2}, they cause the flow to become unicellular, while at lower values a bicellular flow appears.

In summary, it has been shown, for this problem in particular, that a region with important viscous effects at $Da > 10^{-4}$ exists, while as Da decreases, the behavior of the flow becomes closer to the one described by Darcy's law, as has been reported previously in the literature for other geometries. This limit is, in general terms, independent of the particular values of Ra and A. Also, correlations have been proposed to estimate Nu_{med} as a function of Ra, A and Da, for the two cases analyzed. Eqs. (7) and (10) could serve to evaluate, quantitatively, the heat transfer of a problem in particular considering the Darcy number, while Eqs. (8) and (11) could serve for Darcian porous media. However, some experimental data is required to verify the computed flow patterns and isotherms, and the range of validity of those correlations.

Acknowledgement

The authors are grateful for the financial support provided by Consejo Nacional de Ciencia y Tecnología (CONACYT) (Grants 400200-5-4389A and 1231-A9203).

References

[1] R.A. Greenkorn, Flow Phenomena in Porous Media, Marcel Dekker, New York, 1983.
[2] D.A. Nield, A. Bejan, Convection in Porous Media, Springer-Verlag, USA, 1992, Chaps 1 and 7.
[3] A.K. Singh, G.A. Moore, G.R. Thorpe. Macroscope boundary conditions in convective flows in stored grains and other commodities, Conference in Agricultural Engineering, Institute of Engineers of Australia, Toowomba, Queensland, Australia, 1990.
[4] M.A. Havstad, P.J. Burns, Convective heat transfer in vertical cylindrical annuli filled with a porous medium, Int. J. Heat Mass Transfer 11 (1982) 1755–1766.
[5] V. Prasad, A. Chui, Natural convection in a cylindrical

porous enclosure with internal heat generation, J. Heat Transfer 111 (1989) 916–925.
[6] E. David, G. Lauriat, V. Prasad, Non-Darcy natural convection in packed-sphere beds between concentric vertical cylinders, Symposium Series Heat Transfer 85 (1989) 90–95.
[7] M.L. Hunt, C.L. Tien, Non-Darcian convection in cylindrical packed beds, J. of Heat Transfer 110 (1988) 378–384.
[8] Wen-Jeng Chang, Chi-Feng Hsiao, Natural convection in a vertical cylinder filled with anisotropic porous media, Int. J. Heat Mass Transfer 13 (1993) 3361–3367.
[9] H.C. Brinkman, On the permeability of media consisting of closely packed porous particles, Appl. Sci. Res. A1 (1947) 81–86.
[10] J.A. Ochoa-Tapia, S. Whitaker, Momentum transfer at the boundary between a porous medium and a homogeneous fluid—I. Theoretical development, Int. J. Heat Mass Transfer 38 (1995) 2635–2646.
[11] G. Lauriat, V. Prasad, Natural convection in a vertical porous cavity: a numerical study for Brinkman-extended Darcy formulation, J. Heat Transfer 109 (1987) 688–696.
[12] N. Kladias, V. Prasad, Natural convection in horizontal porous layers: effect of Darcy and Prandtl numbers, J. Heat Transfer 111 (1989) 926–935.
[13] P.J. Roache, Computational Fluid Dynamics, Hermosa Publishers, Albuquerque, NM, 1972 Chap. III.
[14] B.A. Finlayson, Nonlinear Analysis in Chemical Engineering, McGraw-Hill, 1980 Chap. 4.
[15] H. Jiménez-Islas, F. López-Isunza, ELI-COL: programa para resolver sistemas de ecuaciones diferenciales parciales elípticas no lineales, por doble colocación ortogonal, Avances en Ingeniería Química 4 (1994) 82–86 México.